



## Oxidation of Phenol by CWPO Method Using Nickel Manganese Oxide Catalyst Prepared in Glycerol Solvent Using Microwave in Batch Reactor

Hadi Falah Hassan<sup>1</sup>, Khaleel I. Hamad<sup>2</sup>, Aysar T. Jarullah<sup>3</sup>

Chemical Engineering Department, College of Engineering, Tikrit University, Tikrit, Iraq

<sup>1</sup>E-mail: [hadi.f.hassan@st.tu.edu.iq](mailto:hadi.f.hassan@st.tu.edu.iq)

<sup>2</sup>E-mail: [Khalil.edan@tu.edu.iq](mailto:Khalil.edan@tu.edu.iq)

<sup>3</sup>E-mail: [a.t.jarullah@tu.edu.iq](mailto:a.t.jarullah@tu.edu.iq)

### ARTICLE INFO

#### Article history:

Received 31 January 2025  
Revised 02 February 2025  
Accepted 22 February 2025  
Available online 22 February 2025

#### Keywords:

Catalytic Wet Peroxide oxidation  
Batch reactor  
Al<sub>2</sub>O<sub>3</sub>/NiMnO<sub>3</sub>  
Oxidant (H<sub>2</sub>O<sub>2</sub>)

### ABSTRACT

Clean, safe, unpolluted water is a growing concern. The petrochemical, pharmaceutical, and hazardous phenols are released into the river by the pulp and paper industries. Therefore, phenol must be removed from polluted water due to its hazardous effects on humans. This study will investigate how phenol can be removed from wastewater by a support nanocomposite catalyst in a batch reactor. By sol-gel technique, nickel and manganese with glycerol were utilized as solvent and Al(NO<sub>3</sub>)<sub>3</sub> as active material to make the nanocatalyst locally and describe it with FTIR, BET, XRD, TEM, and SEM. A novel catalyst was used for catalytic wet peroxide oxidation (CWPO) of phenol. Catalytic tests were done in the batch reactor with an equivalent amount of H<sub>2</sub>O<sub>2</sub>. The CWPO process's working conditions include temperature [40 °C, 50 °C, 60 °C, 70 °C], time [60 min, 80 min, 100 min, 120 min], and beginning phenol concentration [200 ppm]. [1, 300, 400, 500 ppm] at 1 atm. The maximum removal is 92.46% at 70 °C, 120 min, and 200 ppm using (Al<sub>2</sub>O<sub>3</sub>/NiMnO<sub>3</sub>) catalyst.

## 1. Introduction

Phenol, an essential chemical, is utilized in the production of drugs, fungicides, and preservatives and is also an essential product of the petroleum industry. Nevertheless, phenolic compounds are major contaminants that are categorized as carcinogenic and teratogenic materials [1,2]. Due to its dangerous effects in tiny doses, the Environmental Protection Agency (USEPA) has categorized phenol as a priority pollutant, requiring treatment even if a phenol concentration is less than 1 ppm before release[3]. Phenols as environmental pollutants are hazardous to human health and living organisms, owing to their high toxicity levels, and their suspected carcinogens as well

as mutagenic impacts on cells [4]. Phenol at low concentrations of 5–25 mg L<sup>-1</sup> poses a potential carcinogenic risk to human beings, and is fatal to fishes [5]. In the quest to solve this problem different treatments have been studied based on physical and chemical processes (e.g., flocculation, precipitation, adsorption on activated carbon, ozonation, chlorination and coagulation)[6].

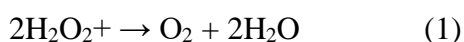
Chemical oxidation is one of the methods that can be used to remove phenol from effluent [7]. AOPs are conceptually characterized by the production of hydroxyl radicals (HO•), which are very reactive species capable to oxidize a wide range of organic compounds and to reduce the toxicity of many effluents. Most of

\* Corresponding author E-mail address: [hadi.f.hassan@st.tu.edu.iq](mailto:hadi.f.hassan@st.tu.edu.iq)  
<https://doi.org/10.61268/1sdyb939>

This work is an open-access article distributed under a CC BY license (Creative Commons Attribution 4.0 International) under

<https://creativecommons.org/licenses/by-nc-sa/4.0/> 

these processes can be operated at (or close to) ambient temperature and atmospheric pressure [8]. Different oxidizing agents (typically hydrogen peroxide, ozone or/and oxygen) can be considered depending on the process [9]. Particularly, hydrogen peroxide ( $H_2O_2$ ) a colorless and non-toxic compound – is a powerful oxidizing agent that easily decomposes into environmentally friendly products (i.e. water and oxygen), following Eq. (1).



The decomposition of ( $H_2O_2$ ) can be selectively advanced by the formation of the highly reactive  $HO\cdot$  radicals when a suitable catalyst is employed. This process is referred to as catalytic moist peroxide oxidation (CWPO). The classical Fenton process is a well-known homogeneous AOP that utilizes a mixture of ( $H_2O_2$ ) and  $Fe^{2+}$  ions at a low pH (2.5 - 3.0) to facilitate the decomposition of ( $H_2O_2$ ) into  $HO\cdot$  radicals. This process is considered a specific example of CWPO, which pertains to a specific catalyst under specific operating conditions. Even so, heterogeneous catalysts are more easily separated from the treated solution than homogeneous catalysts [10]. Catalysts are employed to implement catalytic wastewater treatment processes through oxidation, resulting in a decrease in activation energy and the process occurring under moderate conditions. Furthermore, ( $H_2O_2$ ) is employed as an oxidant in the catalytic oxidation process to circumvent the constraints of liquid–gas mass transfer and significantly enhance the process's efficiency [11]. Currently, nanomaterials are extensively employed in a variety of environmental treatment applications due to their distinctive physiochemical properties. At the economic level, nanotechnology is advantageous for the conservation of energy and the utilization of water resources. In addition, nanostructured adsorbents are utilized for wastewater treatment due to their greater efficiency and quicker reaction rate [12]. The sol-gel method was employed to prepare a novel nanocatalyst,  $Al(NO_3)_3 \cdot 9H_2O$ , which serves as the active

metal. Additionally,  $NiMnO_3$  ( $Al_2O_3/NiMnO_3$ ) was synthesized using glycerol as the solvent due to the high activity of improving catalyst structure and eventually the stability [13,14], glycerol was used in our study to emphasize its durability on oil industry [15]. A batch reactor was used in this study to remove phenol from wastewater. Hydrogen peroxide was employed to expedite the catalytic oxidation of phenol. Subsequently, the reactor and catalyst were assessed for efficacy by conducting a series of experiments under varying operating conditions. The optimization process was executed to determine the optimal parameters for the catalytic phenol oxidation process, thereby maximizing phenol removal. The unique aspect of this study is that the catalytic phenol oxidation process was conducted in the presence of a home-made nanocatalyst ( $Al_2O_3/NiMnO_3$ )

## 2. Materials and methods

### 2.1 Material Application

#### 2.1.1 Feedstock

The raw material was a typical sewage water prepared by injecting phenol at different concentrations 100-500 mg/L into demineralized water where phenol was supplied by (The E-Merck company in India, with 99% purity).

#### 2.1.2 Hydrogen Peroxide (35% $H_2O_2$ )

$H_2O_2$  (Sigma-Aldrich (Germany), purity above 99.99%) was utilized to oxidize phenol to  $CO_2$  and  $H_2O$

#### 2.1.3 Glycerol

Thanks to its unique physical and chemical properties, glycerol is an excellent solvent in many chemical and industrial applications. the properties of glycerol supplied by CARLO ERBA in Italy.

### 2.2 Catalyst

#### 2.2.1 Aluminum Nitrate Nonahydrate

Aluminum Nitrate Nonahydrate ( $\text{Al}(\text{NO}_3)_3 \cdot 9\text{H}_2\text{O}$ ) (obtained from company LOBA CHEMIE PVT, India) was employed as the active metal in the nano-catalyst that was developed ( $8\% \text{ Al}_2\text{O}_3/\text{NiMnO}_3$ ). with purity 98%

### 2.2.2 Support

The following Table specifies the Support:

**Table 1:** Support materials specification

No.	Support	Precursor	Catalyst	Supplying company	Purity %
1	Ni	$\text{C}_4\text{H}_6\text{NiO}_4 \cdot 4\text{H}_2\text{O}$	$\text{Al}_2\text{O}_3/\text{NiMnO}_3$	Sisco Research Laboratories Pvt. Ltd., India	98%
2	Mn	$\text{C}_4\text{H}_7\text{MnO}_4 \cdot 4\text{H}_2\text{O}$	$\text{Al}_2\text{O}_3/\text{NiMnO}_3$	Sigma Aldrich, Germany	99%

### 2.3 Catalyst preparation

Metal oxides were prepared by mixing nickel and manganese in glycerol using sol-gel technique, where equal amounts of nickel and manganese were added with 5 times the amount of glycerol i.e. 1:5 nickel and manganese to glycerol in a vessel for 16 h at 200 °C using a magnetic stirring system sample was taken and placed in a drying oven for a whole day at 120 °C .microwave-assisted calcination was also implemented as. The flask was then placed in a microwave reactor system and microwave calcinated for 7 minutes at 80% power with a low stirring speed. The initial wetting impregnation (IWI) method was used to load  $\text{Al}(\text{NO}_3)_3 \cdot 9\text{H}_2\text{O}$ . The target loading is 8%  $\text{Al}_2\text{O}_3/\text{NiMnO}_3$ . 24 g of Al was dissolved in To guarantee the complete dissolution of the active material in the solvent, 50 ml of deionized water was stirred in a magnetic stirrer for 60 minutes. Then, the active material is produced solution was slowly added to 20 g of the support (Ni-MnO) with continuous stirring for 180 min to ensure complete dispersion of the active metal on the support. The sample was dried for 4 h at 100 °C in an oven. The sample was prepared after being loaded by the impregnation method and. Microwave-assisted calcination was also conducted. The flask was then placed in a microwave reactor system, 80% power for 7 minutes with a low stirring motion.

### 2.4 Catalytic oxidation of phenol

The catalytic oxidation of phenol in the model solution for phenol treatment was

conducted on the locally designed nano catalyst using  $\text{H}_2\text{O}_2$  as the oxidant (25 mL contaminated water/1 mL  $\text{H}_2\text{O}_2$ ). This was done to evaluate the performance of the nano catalyst. The initial phenol concentration was injected into the model solution (200, 300, 400 and 500 mg/L) of phenol as a model of phenolic compounds. in a three-necked bottle, 1 g of nano catalyst was charged. A 100 ml sample of raw material was taken into the batch reactor for each cycle of catalytic oxidation of phenol. For each experiment, the catalyst weight was 1 g, and the raw materials to oxidant ( $\text{H}_2\text{O}_2$ ) ratio was 25. phenol underwent catalytic oxidation under moderate conditions, with an oxidation time of 60, 80, 100, and 120 minutes and a reaction temperature of 40, 50, 60, and 70 °C. The rate of airflow is 100 L/h, and A constant pressure of 1 atm was employed in all instances. In the course of the chemical reaction, gases were evaporated and subsequently condensed. The reaction mixture was cooled to room temperature and the catalyst was separated from the oxidant-phenol solution by filtration after each oxidation reaction cycle. An estimation of the final phenol concentration was conducted by utilizing UV spectrometry to analyze the treated product.

### 2.5 UV Spectrophotometer Analysis

UV-visible spectroscopy proved ideal for phenolic and phenol chemicals in model solution. In fact, two factors determined chemical concentration. Firstly, UV light absorbs phenol and phenolic chemicals. Second, colored compounds, which could absorb visible

light, were estimated. The wavelength of phenol was 269 nm.

### 3. Results and discussion

#### 3.1 BET

The Brunauer–Emmett–Teller (BET) test examined surface area, pore volume, and pore size of  $\text{Al}_2\text{O}_3/\text{NiMnO}_3$ . Table 2 shows the

results. The nano-catalyst ( $\text{Al}_2\text{O}_3/\text{NiMnO}_3$ ) surface area and pore volume were important in catalytic oxidation. Increased surface area increased phenol elimination. Large surface area provided efficient phenol  $\text{H}_2\text{O}_2$  interaction, resulting in significant phenol elimination. The large surface area also helped phenol molecules reach the catalyst's surface-active regions.

**Table 2:** Surface area and pore volume information for catalyst

Property	Nano-Catalyst ( $\text{Al}_2\text{O}_3/\text{NiMnO}_3$ )
Surface area, ( $\text{m}^2/\text{g}$ )	189.36
pore volume, $\text{cm}^3/\text{g}$	0.137
Pore size, nm	2.110

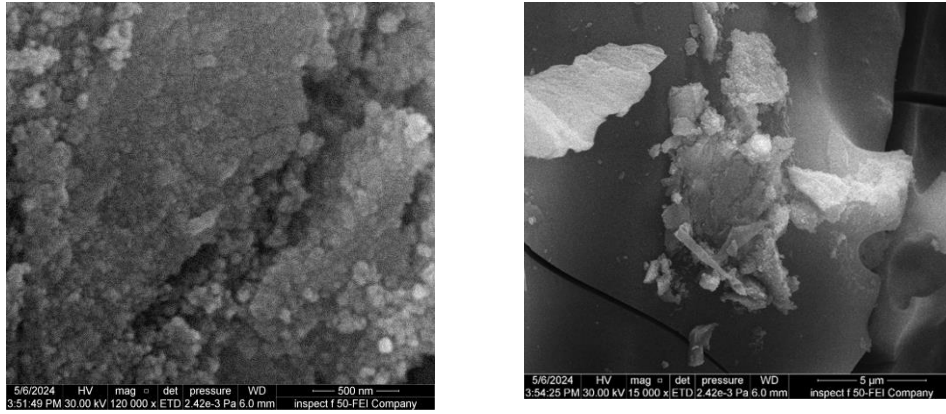
#### 3.2 SEM-EDX

Figure (1) depicts ( $\text{Al}_2\text{O}_3/\text{NiMnO}_3$ ) composite nanostructure FESEM images. Nanostructures were 30.22–58.73 nm. The absorbent material was able to provide the best surface area for phenol adsorption due to the varied pore sizes [16]. The images showed how microwave energy shapes nanostructures. The smaller, closer-spaced particles of microwave radiation accelerate and lower the cost of chemical reactions. The images show nanoparticles. . Due to microwave reactor heating speed and efficiency. Rapid heating shrinks nanoparticles and reduces agglomerations, ensuring uniformity. Rapid heating forms particles quickly, limiting crystal growth and reducing nanoparticle size. This is due to low calcination interparticle interaction[17, 18].

The study reveals that glycerol as a solvent for preparation can allow early crystal structure ordering. Glycerol's strong polarity allows tiny molecules to adsorb and promotes nanomaterial

chemical reactions. Glycerol improves catalytic applications by increasing adsorption capacity [19]. The utilization of aluminum nitrate as a support or carrier for nanoparticles results in an increase in the effective surface area of the nanoparticles, which in turn enhances their efficiency in catalytic applications [20]. The EDX elemental analysis of the ( $\text{Al}_2\text{O}_3/\text{NiMnO}_3$ ) composite is illustrated in Figure (2). The analysis indicates that the composite is composed of a blend of elements in varying weight percentages, such as nickel (21.9%), manganese (22.8%), oxygen (31.4%), and aluminum (13.7%). These elements are the primary components used in the composite's production. Carbon (14.6%), fluoride (3.0%), and silicon (0.1%) are among the additional peaks. The EDX image illustrates a consistent and efficient dispersion of active metal on the nano-catalyst's surface. The theoretical calculations of the manganese, nickel, and aluminum amounts in the nano-catalyst that was designed are in good agreement with the results.





**Figure 1:** FESEM images of  $\text{Al}_2\text{O}_3/\text{NiMnO}_3$

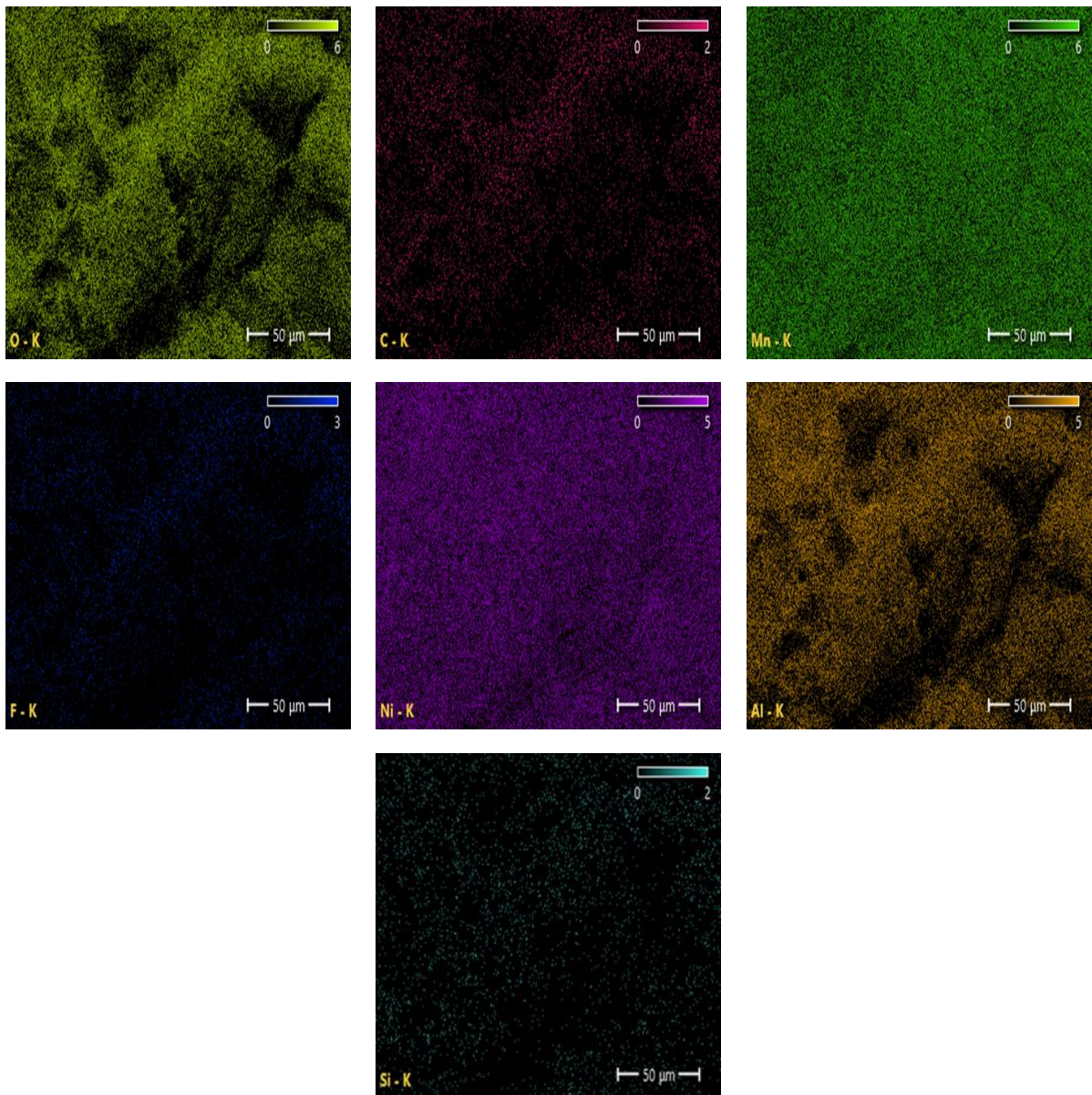


**Figure 2:** EDX mapping analysis  $\text{Al}_2\text{O}_3/\text{NiMnO}_3$

### 3.3 XRD

The (Al<sub>2</sub>O<sub>3</sub>/NiMnO<sub>3</sub>) composite's crystalline nature, average particle size, and interatomic layer spacing were determined by XRD analysis Figure (3). The broad peaks suggest tiny crystals and overlap between many compounds' peaks. Unambiguous diffraction peak at  $2\theta = 44^\circ$  and

peak width (1.0154) in the XRD spectrum show a percentage of crystalline nature. Overlapping peaks in the spectrum indicate semi-crystalline materials. In the Scherrer equation, 47 nm is the crystal size. Fast microwave calcination produces high temperatures, which explains this result. This stops crystals from growing, creating a dilute structure with little crystals [21].

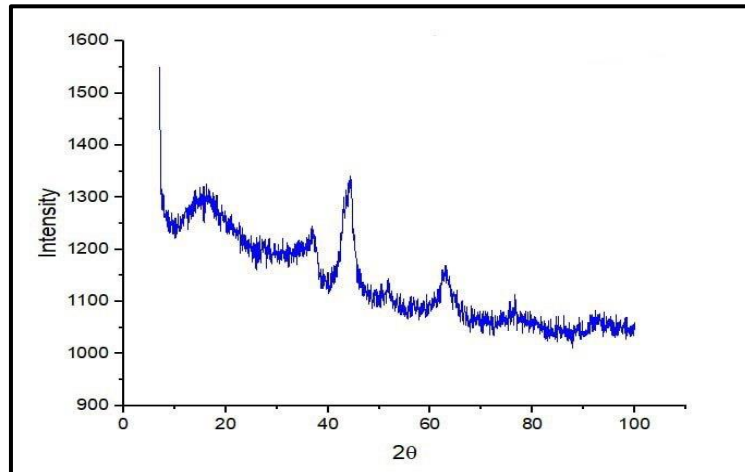


**Figure 3:** X-ray diffraction patterns of Al<sub>2</sub>O<sub>3</sub>/NiMnO<sub>3</sub> composite

### 3.4 FTIR

The samples were analyzed within the 500-4000 cm<sup>-1</sup> spectral range as shown in the figure (4). The presence of hydroxyl groups (-OH) is indicated by the pronounced absorption observed in the 3000-3200 cm<sup>-1</sup> range, which can be attributed to O-H absorption vibrations [22]. This may be the result of glycerol or water adsorbed on the surface. Symmetric and asymmetric C-H vibrations are indicated in glycerol or any other organic compound within the 3000-2800 cm<sup>-1</sup> range. The range of 1600-1400 cm<sup>-1</sup> Absorption peaks are observed in this range, which may be attributed to the presence of C=O or C=C vibrations in organic materials or to the formation of metallic compounds, such as aluminum nitrate, which contain N-O bonds. 1100-1000 cm<sup>-1</sup> C-O-C or P-O-C vibrations may be indicated by absorption peaks in this region. This could suggest the presence of organic materials or compounds containing phosphorus. Less than 1000 cm<sup>-1</sup>. The occurrence of numerous peaks in this range is

indicative of the formation of metallic oxides as a consequence of calcination processes, as it can be attributed to the vibrations of metallic oxygen such as Ni-O and MnO.

### 3.5 TGA

The (Al<sub>2</sub>O<sub>3</sub>/NiMnO<sub>3</sub>) catalyst thermo gravimetric curves are shown TGA curves show transpired decomposed in three phases. The relative stability in weight observed as a result of moisture elimination during heating from 25 to 250 °C suggests that glycerol evaporation has completed and light organics are decomposing [23]. In the second stage of breakdown between 250 and 488 °C, weight loss was 5.05%. At thermal treatment temperatures, heavier organics or residual chemicals decompose. In the third stage, which begins at 488-600 °C, weight stability indicates the completion of breakdown and mineral structure stabilisation. Small weight loss and quasi-steady mass loss at temperatures above 600 °C indicate that the element's essential structure has consolidated [24]

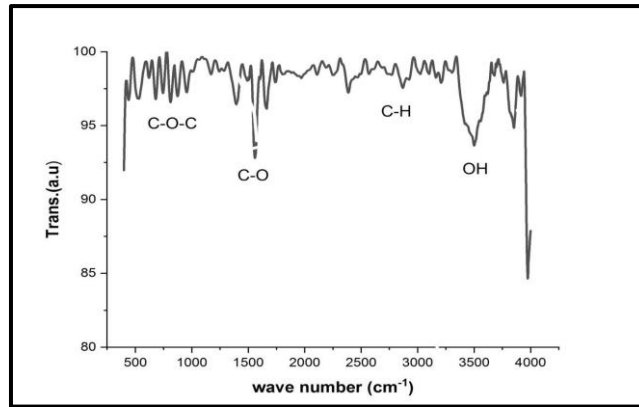


**Figure (4):** FTIR spectra of catalyst

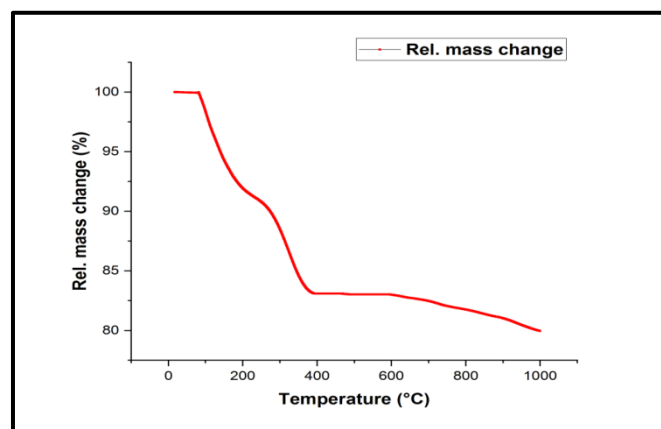


**Figure 5:** TGA for the catalysts of Al<sub>2</sub>O<sub>3</sub>/NiMnO<sub>3</sub> composite

**3.6 Effect of operating conditions on the catalytic phenol oxidation process**

The removal of phenol from effluent by oxidation reaction was investigated at 40 °C, 50°C, 60°C, and 70°C. The results were visually represented in Figures (6 to 9) at various temperatures.

**3.6.1 Effect of reaction temperature**

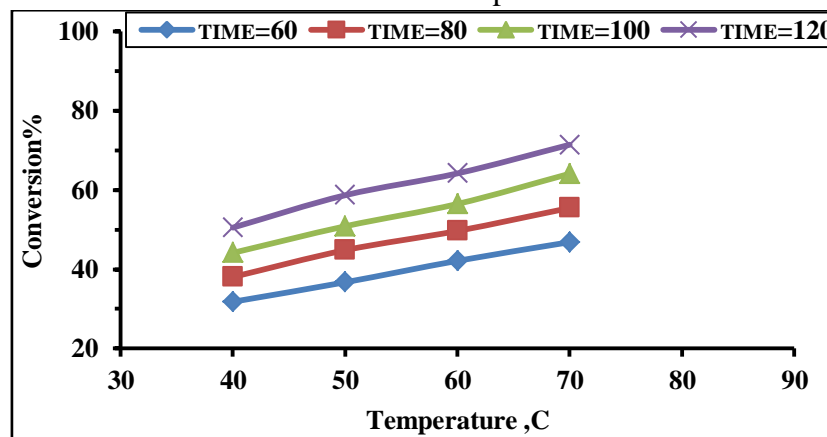


**Figure 6:** Effect of temperature on phenol oxidation at initial phenol concentration, 500 ppm

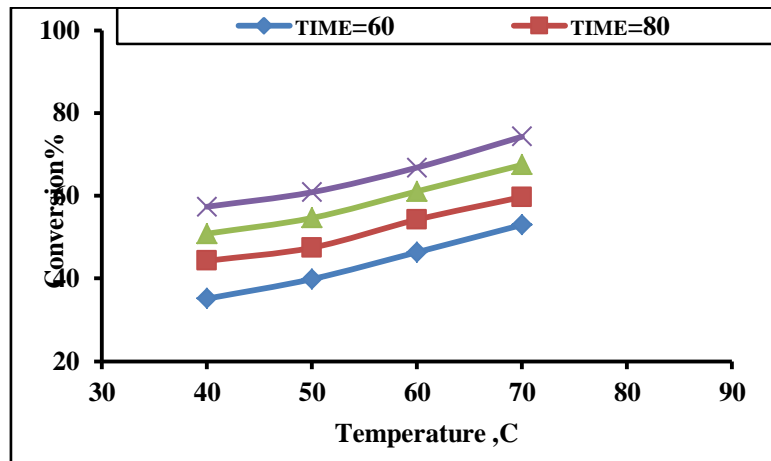


**Figure 7:** Effect of temperature on phenol oxidation at initial phenol concentration, 400 ppm

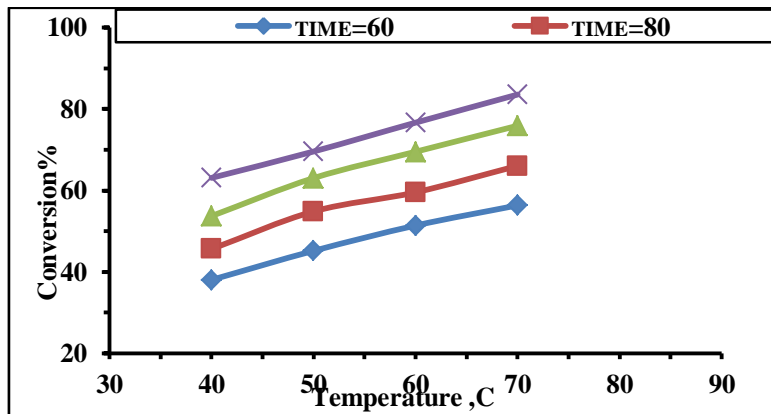


**Figure 8:** Effect of temperature on phenol oxidation at initial phenol concentration, 300 ppm

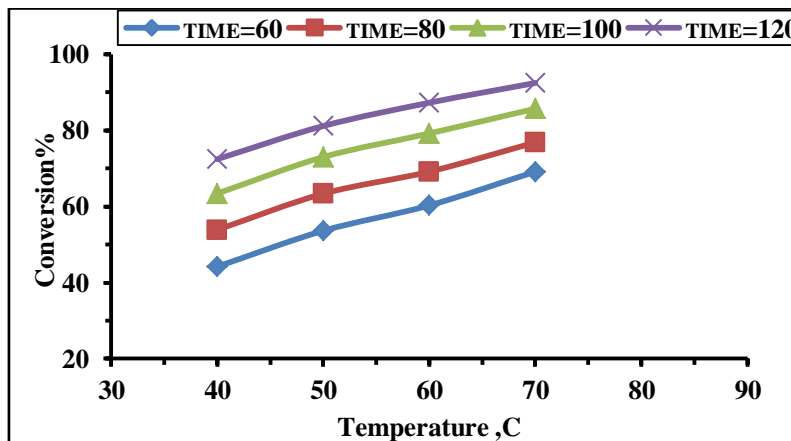


**Figure 9:** Effect of temperature on phenol oxidation at initial phenol concentration, 200 ppm

The decomposition of hydrogen peroxide ( $H_2O_2$ ) in the water is facilitated by an increase in temperature, which in turn increases the efficiency of phenol removal from polluted

water. This process also contributes to the oxidation reaction and decomposition of organic pollutants by generating hydroxyl free radicals. The most effective temperature for phenol



oxidation is 70°C, as hydrogen peroxide begins to decompose and loses its oxidant properties beyond this point [25]. Under optimal operating conditions, which included a reaction temperature of 70 °C and a residence time of 120 minutes, the (Al<sub>2</sub>O<sub>3</sub>/NiMnO<sub>3</sub>) nanocatalyst was found to have a maximal phenol removal efficiency of 92.46%. An enhanced phenol decomposition reaction is the result of increasing the temperature. The oxidation efficacy is enhanced at elevated temperatures as a result of the increased production of free radicals (namely, hydroxyl radicals) from the decomposition of hydrogen peroxide (H<sub>2</sub>O<sub>2</sub>). The phenol is broken down into simpler compounds by these free radicals, which are potent oxidizing agents. Eventually, the phenol is converted into water, carbon dioxide, and metal salts during the "mineralization" cycle.

The efficacy of the Nano catalysts, such as (Al<sub>2</sub>O<sub>3</sub>/NiMnO<sub>3</sub>), is also enhanced by increasing the temperature. The surface of the catalysts undergoes enhanced oxidation reactions and increased molecular movement as a result of heat. The oxidation efficacy is also improved by the increase in the contact area between phenol and free radicals, which is facilitated by heat. Nevertheless, the efficacy of hydrogen peroxide is diminished as a result of its decomposition at temperatures exceeding 70 °C [26].

### 3.6.2 Effect of reaction time

The oxidation reaction was implemented to examine the influence of time on the effluent's phenol removal at 60, 80, 100, and 120 minutes. The experimental data are presented in figures (10 to 13) at various time intervals.

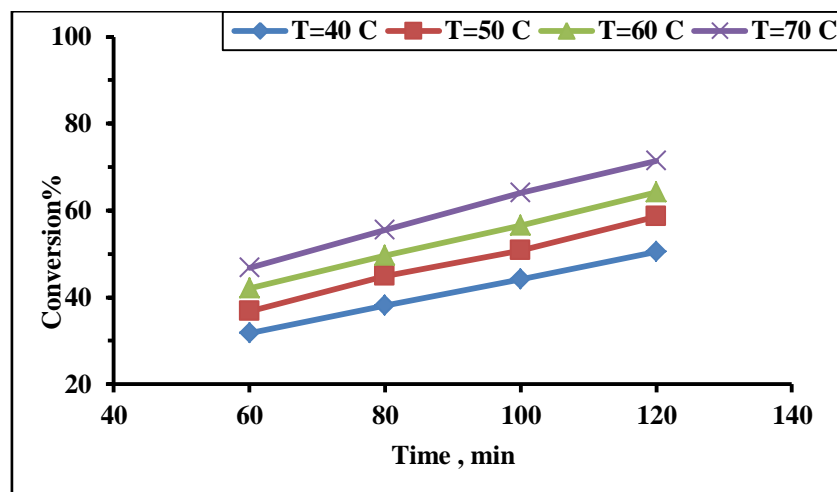


**Figure10:** Effect of time on phenol oxidation at initial phenol concentration, 500 ppm

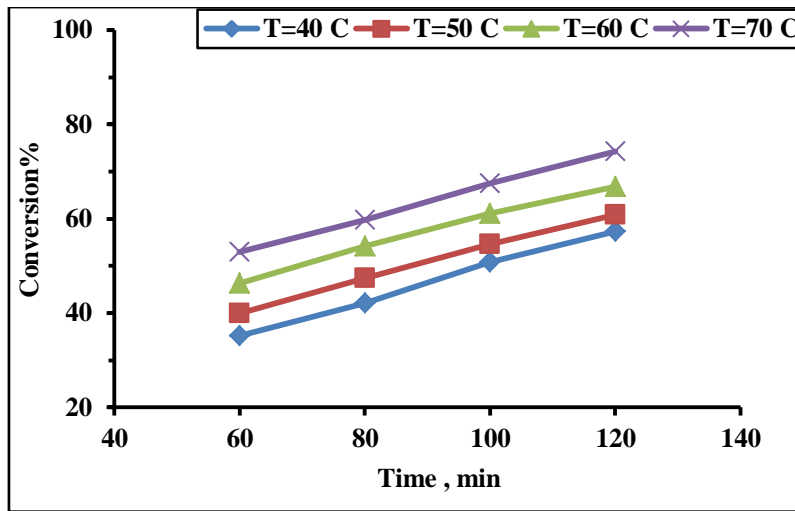


Figure 11: Effect of time on phenol oxidation at initial phenol concentration, 400 ppm

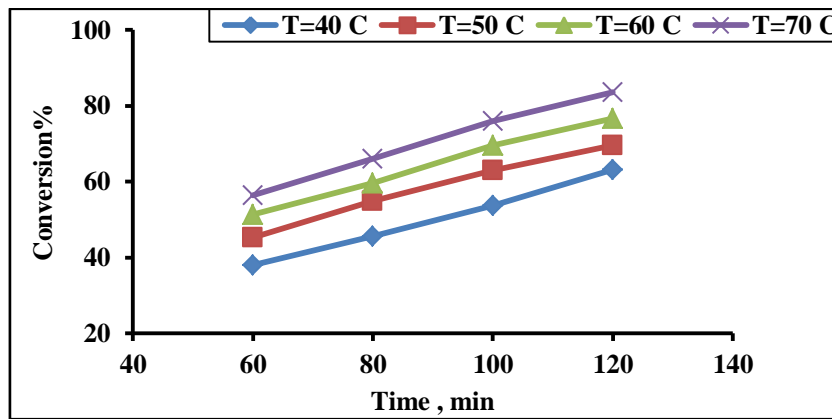


Figure 12: Effect of time on phenol oxidation at initial phenol concentration, 300 ppm

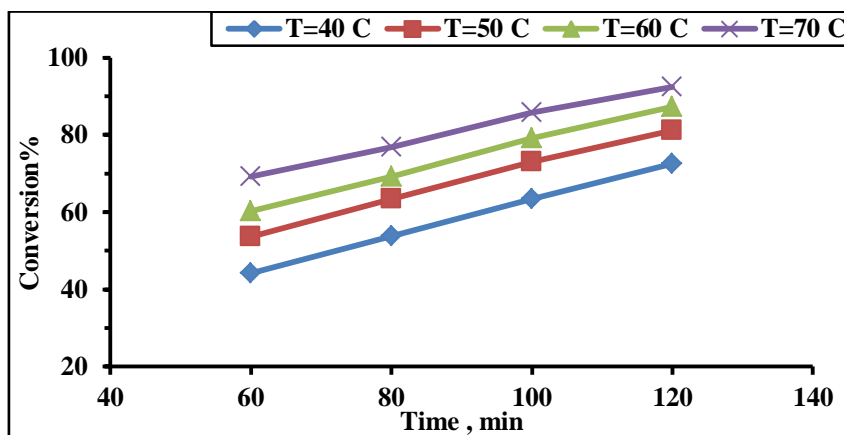


Figure 13: Effect of time on phenol oxidation at initial phenol concentration, 200 ppm

From Figures 10 to 13, it is evident that the efficacy of phenol removal from water using Nano catalysts is significantly influenced by the reaction time at the outset. The oxidation reaction is enhanced, and the removal of phenol into less harmful products is facilitated by an increase in reaction time. This behavior may be attributed to the return to a rapid adsorption (physically) on the surface of  $(Al_2O_3/NiMnO_3)$ , which led to the initial removal of phenol. The process of phenol oxidation was progressively improved as the duration of time increased [27]. Figures 11 to 14 also demonstrate that the oxidation efficiency of phenol increases significantly as the reaction time increases up to 120 minutes. At this point, the process reaches a steady state, as there is no significant

improvement in the removal efficiency after this point. This suggests that the majority of the phenol has been oxidized and converted into simpler substances, and that increasing the time after this period may not have a significant effect, as the oxidation process has reached its highest efficiency. Consequently, the highest phenol removal rate of up to 92% was achieved using  $(Al_2O_3/NiMnO_3)$  at a temperature of 70 °C [28].

### 3.6.3 Effect of initial phenol concentration

The removal of phenol from effluent through an oxidation reaction was investigated in relation to the initial concentration at 200 ppm, 300 ppm, 400 ppm, and 500 ppm are depicted in Figures 14 to 17 under varying conditions.

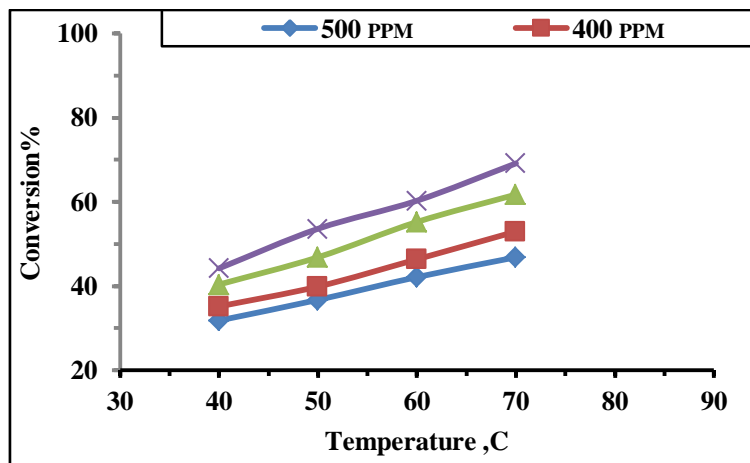


Figure 14: Effect of initial phenol concentration on phenol oxidation at time =60 min

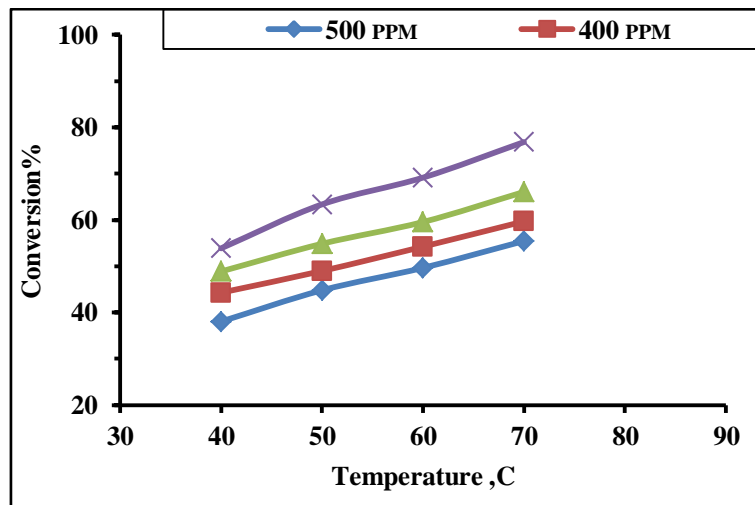
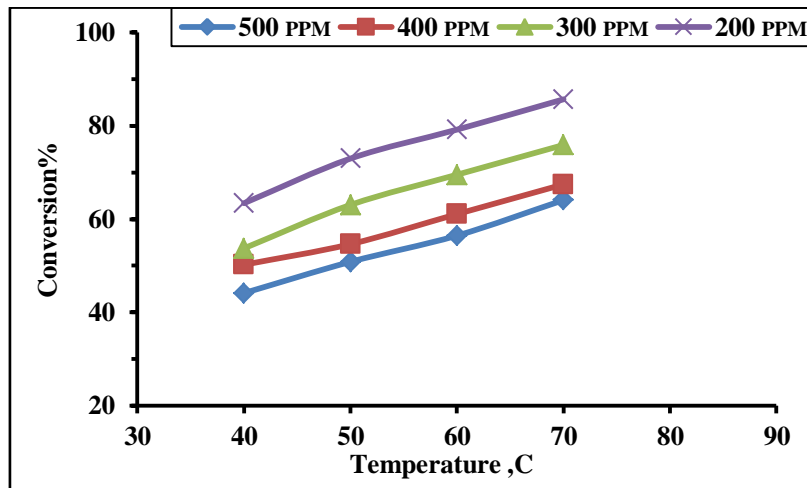
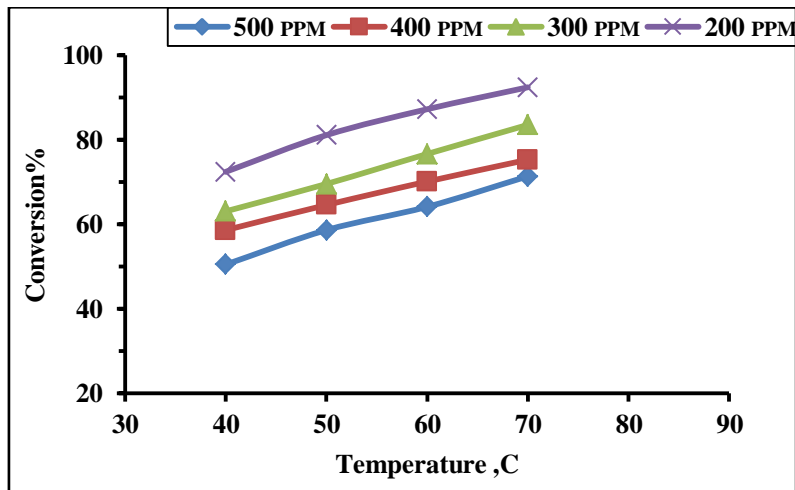


Figure 15: Effect of initial phenol concentration on phenol oxidation at time, 80 min



**Figure 16:** Effect of initial phenol concentration on phenol oxidation at time 100 min



**Figure 17:** Effect of initial phenol concentration on phenol oxidation at time 120 min

At different initial concentrations of phenol (200, 300, 400, and 500 mg/L), Figure (17) shows the rates of phenol degradation. The rate of phenol removal increases with decreasing phenol concentration, as shown in the graph. One can notice that at lower initial phenol concentration, there is a faster and more efficient reaction with the catalyst. Because the active sites on the catalyst surface are not completely saturated, the catalyst can handle  $H_2O_2$  and the  $H_2O_2$  molecules decompose into hydroxyl radicals through a catalytic reaction where hydroxyl radicals break the bonds in the phenol molecules and convert them into less complex intermediate compounds with higher efficiency

and achieve a complete or almost complete oxidation reaction. As the phenol concentration increases, the reaction remains efficient, but the efficiency begins to decrease because the active sites on the catalyst approach saturation, which reduces the oxidation efficiency. In this case, the catalyst may not be able to handle all the phenol in the specified time. ( $Al_2O_3/NiMnO_3$ ) catalyst and  $H_2O_2$  were used as oxidant at 70 °C for 120 min. The removal rates were 92.46% and 83.57% when the phenol concentration increased from 200 to 300 mg/L, and decreased from 83.57% to 71.39% when the phenol concentration increased from 300 to 500 mg/L. The results of the present investigation were

consistent with the results of Noora A. Raheem[29], Huda Adil Sabbar[30], and Hayder A.K. Al-jandeel[31]. As the phenol content increases, the removal efficiency decreases. The role of hydrogen peroxide ( $H_2O_2$ ) in the CWPO process is as a major oxidant that produces active hydroxyl radicals that degrade organic compounds. The success of the oxidation depends largely on the appropriate dosage of  $H_2O_2$  as well as on the effectiveness of the catalyst ( $Al_2O_3/NiMnO_3$ ) to catalyze the decomposition of  $H_2O_2$  into hydroxyl radicals.

#### 4. Conclusions

In order to optimize the catalytic phenol oxidation process in a batch reactor by employing hydrogen peroxide as an oxidant., a novel nanocatalyst was developed through the sol-gel technique with glycerol as the solvent. As indicated by scanning electron microscopy, the metal oxide disseminated on the catalyst exhibited a high morphology. The porosity of the prepared nanocatalyst was evidenced by the phenol oxidation process, which was influenced by the same base of active metal oxides ( $Al(NO_3)_3$ ) on the surfaces of these absorbents (nickel manganese oxide). Under moderate operating conditions (reaction temperature 70 °C, reaction time 120 min, and initial phenol concentration 200 ppm), the fabricated nanocatalyst ( $Al_2O_3/NiMnO_3$ ) was detected to be an effective adsorbent for the phenolic compound, resulting in the removal of 92.46% of phenol . The utilization of nanoparticles to produce the catalyst demonstrated exceptional performance in the CWPO phenol removal process. The sol-gel method is an effective technique for the preparation of the nanocatalyst because of the enhanced dispersion of the active metal, as well as the high pore volume and surface area of the catalyst ( $Al_2O_3/NiMnO_3$ ). Mainly, the efficacy is contingent upon the active compound and the quantity of metal oxide that is loaded onto the catalyst support (Ni-MnO)

#### References

- [1] B. Iurascu, I. Siminiceanu, D. Vione, M. A. Vicente, and A. Gil, "Phenol degradation in water through a heterogeneous photo-Fenton process catalyzed by Fe-

- treated laponite," *Water Res.*, vol. 43, no. 5, pp. 1313–1322, 2009, doi: 10.1016/j.watres.2008.12.032.
- [2] S. Zhang *et al.*, "Efficient Treatment of Phenol Wastewater by Catalytic Ozonation over Micron-Sized Hollow MgO Rods," *ACS Omega*, vol. 6, no. 39, pp. 25506–25517, 2021, doi: 10.1021/acsomega.1c03497.
- [3] R. N. Abbas and A. S. Abbas, "Kinetics and Energetic Parameters Study of Phenol Removal from Aqueous Solution by Electro-Fenton Advanced Oxidation Using Modified Electrodes with PbO<sub>2</sub> and Graphene," *Iraqi J. Chem. Pet. Eng.*, vol. 23, no. 2, pp. 1–8, 2022, doi: 10.31699/ijcpe.2022.2.1.
- [4] X. Quan, H. Shi, H. Liu, J. Wang, and Y. Qian, "Removal of 2, 4-dichlorophenol in a conventional activated sludge system through bioaugmentation," *Process Biochem.*, vol. 39, no. 11, pp. 1701–1707, 2004.
- [5] S. C. Atlow, L. Bonadonna-Aparo, and A. M. Klibanov, "Dephenolization of industrial wastewaters catalyzed by polyphenol oxidase," *Biotechnol. Bioeng.*, vol. 26, no. 6, pp. 599–603, 1984.
- [6] G. Busca, S. Berardinelli, C. Resini, and L. Arrighi, "Technologies for the removal of phenol from fluid streams: a short review of recent developments," *J. Hazard. Mater.*, vol. 160, no. 2–3, pp. 265–288, 2008.
- [7] D. He, X. Guan, J. Ma, and M. Yu, "Influence of different nominal molecular weight fractions of humic acids on phenol oxidation by permanganate," *Environ. Sci. Technol.*, vol. 43, no. 21, pp. 8332–8337, 2009.
- [8] R. Andreozzi, V. Caprio, A. Insola, and R. Marotta, "Advanced oxidation processes (AOP) for water purification and recovery," *Catal. today*, vol. 53, no. 1, pp. 51–59, 1999.
- [9] L. F. Liotta, M. Gruttadauria, G. Di Carlo, G. Perrini, and V. Librando, "Heterogeneous catalytic degradation of phenolic substrates: catalysts activity," *J. Hazard. Mater.*, vol. 162, no. 2–3, pp. 588–606, 2009.
- [10] N. S. Inchaurredo, P. Massa, R. Fenoglio, J. Font, and P. Haure, "Efficient catalytic wet peroxide oxidation of phenol at moderate temperature using a high-load supported copper catalyst," *Chem. Eng. J.*, vol. 198, pp. 426–434, 2012.
- [11] Y. Yan, X. Wu, and H. Zhang, "Catalytic wet peroxide oxidation of phenol over Fe<sub>2</sub>O<sub>3</sub>/MCM-41 in a fixed bed reactor," *Sep. Purif. Technol.*, vol. 171, pp. 52–61, 2016, doi: 10.1016/j.seppur.2016.06.047.
- [12] P. Jangid and M. P. Inbaraj, "Applications of nanomaterials in wastewater treatment," *Mater. Today Proc.*, vol. 43, pp. 2877–2881, 2021, doi: 10.1016/j.matpr.2021.01.126.
- [13] J. Zhang, G. Singh, S. Xu, K. Hamad, A. Ratner, and Y. Xing, "A scalable approach of using biomass derived glycerol to synthesize cathode materials for lithium-ion batteries," *J. Clean. Prod.*, vol. 271, pp. 1–25, 2020, doi: 10.1016/j.jclepro.2020.122518.
- [14] J. Zhang, S. Xu, K. I. Hamad, A. M. Jasim, and Y. Xing, "High retention rate NCA cathode powders from spray drying and flame assisted spray pyrolysis



- using glycerol as the solvent,” *Powder Technol.*, vol. 363, pp. 1–6, 2020.
- [15] K. I. Hamad and Y. Xing, “Effect of Cobalt and Nickel Contents on the Performance of Lithium Rich Materials Synthesized in Glycerol Solvent,” *J. Electrochem. Soc.*, vol. 165, no. 11, pp. A2470–A2475, 2018, doi: 10.1149/2.0311811jes.
- [16] A. Ali, M. Bilal, R. Khan, R. Farooq, and M. Siddique, “Ultrasound-assisted adsorption of phenol from aqueous solution by using spent black tea leaves,” *Environ. Sci. Pollut. Res.*, vol. 25, no. 23, pp. 22920–22930, 2018, doi: 10.1007/s11356-018-2186-9.
- [17] N. Assi, P. A. Azar, M. S. Tehrani, and S. W. Husain, “Studies on photocatalytic performance and photodegradation kinetics of zinc oxide nanoparticles prepared by microwave-assisted sol–gel technique using ethylene glycol,” *J. Iran. Chem. Soc.*, vol. 13, no. 9, pp. 1593–1602, 2016, doi: 10.1007/s13738-016-0875-1.
- [18] R. Al-Gaashani, S. Radiman, N. Tabet, and A. R. Daud, “Effect of microwave power on the morphology and optical property of zinc oxide nano-structures prepared via a microwave-assisted aqueous solution method,” *Mater. Chem. Phys.*, vol. 125, no. 3, pp. 846–852, 2011, doi: 10.1016/j.matchemphys.2010.09.038.
- [19] K. I. Hamad, J. Y. Liao, T. W. Smith, and Y. Xing, “Synthesis of Layered LiMn1/3Ni1/3Co1/3O2 Oxides for Lithium-Ion Batteries using Biomass-Derived Glycerol as Solvent,” *Energy Technol.*, vol. 6, no. 4, pp. 710–717, 2018, doi: 10.1002/ente.201700646.
- [20] W. A. Wan Abu Bakar, R. Ali, and N. S. Mohammad, “The effect of noble metals on catalytic methanation reaction over supported Mn/Ni oxide based catalysts,” *Arab. J. Chem.*, vol. 8, no. 5, pp. 632–643, 2015, doi: 10.1016/j.arabjc.2013.06.009.
- [21] F. Majid, S. Riaz, and S. Naseem, “Microwave-assisted sol–gel synthesis of BiFeO<sub>3</sub> nanoparticles,” *J. Sol-Gel Sci. Technol.*, vol. 74, no. 2, pp. 310–319, 2015, doi: 10.1007/s10971-014-3477-3.
- [22] M. Hadj-Sadok Ouaguenouni, A. Benadda, A. Kiennemann, and A. Barama, “Preparation and catalytic activity of nickel-manganese oxide catalysts in the reaction of partial oxidation of methane,” *Comptes Rendus Chim.*, vol. 12, no. 6–7, pp. 740–747, 2009, doi: 10.1016/j.crci.2008.12.002.
- [23] X. Wu, L. Liu, J. Liu, B. Hou, Y. Du, and X. Xie, “NiMn mixed oxides with enhanced low-temperature deNO<sub>x</sub> performance: Insight into the coordinated decoration of MnO<sub>x</sub> by NiO phase via glycine combustion method,” *Appl. Catal. A Gen.*, vol. 610, 2021, doi: 10.1016/j.apcata.2020.117918.
- [24] Y. Lei, X. Lin, and H. Liao, “Effect of Ni, Fe and Mn in different proportions on microstructure and pollutant-catalyzed properties of Ni-Fe-Mn-O negative temperature coefficient ceramic nanocompositions,” *Mater. Chem. Phys.*, vol. 194, pp. 128–136, 2017, doi: 10.1016/j.matchemphys.2017.03.024.
- [25] S. A. Jafar, A. T. Nawaf, and J. I. Humadi, “Improving the extraction of sulfur-containing compounds from fuel using surfactant material in a digital baffle reactor,” *Mater. Today Proc.*, vol. 42, pp. 1777–1783, 2021, doi: 10.1016/j.matpr.2020.11.821.
- [26] R. J. Issa, Yousif S. Hamad, Khaleel I. Algawi and A. K. Humadi, Jasim I. Al-Salihi, Sara Ahmed, Mustafa A. Hassan, Ahmed A. Abd Jasim, “Removal efficiency and reaction kinetics of phenolic compounds in refinery wastewater by nano catalytic wet oxidation,” *Int. J. Renew. Energy Dev.*, vol. 12, no. 3, pp. 508–519, 2023, doi: 10.14710/ijred.2023.52044.
- [27] K. I. Hamad, J. I. Humadi, Y. S. Issa, S. A. Gheni, M. A. Ahmed, and A. A. Hassan, “Enhancement of activity and lifetime of nano-iron oxide catalyst for environmentally friendly catalytic phenol oxidation process,” *Clean. Eng. Technol.*, vol. 11, no. August, p. 100570, 2022, doi: 10.1016/j.clet.2022.100570.
- [28] A. T. Nawaf, J. I. Humadi, A. T. Jarullah, M. A. Ahmed, S. A. Hameed, and I. M. Mujtaba, “Design of Nano-Catalyst for Removal of Phenolic Compounds from Wastewater by Oxidation Using Modified Digital Basket Baffle Batch Reactor: Experiments and Modeling,” *Processes*, vol. 11, no. 7, 2023, doi: 10.3390/pr11071990.
- [29] N. A. Raheem, N. S. Majeed, and Z. Al Timimi, “Phenol Adsorption from Simulated Wastewater Using Activated Spent Tea Leaves,” *Iraqi J. Chem. Pet. Eng.*, vol. 25, no. 1, pp. 95–102, 2024, doi: 10.31699/ijcpe.2024.1.9.
- [30] H. Adil Sabbar, “Adsorption of Phenol from Aqueous Solution using Paper Waste,” *Iraqi J. Chem. Pet. Eng.*, vol. 20, no. 1, pp. 23–29, 2019, doi: 10.31699/ijcpe.2019.1.4.
- [31] H. A.K. Al-jandeel, “Removal of Phenolic Compounds from Aqueous Solution by Using Agricultural Waste (Al-Khriet),” *Iraqi J. Chem. Pet. Eng.*, vol. 14, no. 3, pp. 55–62, 2013, doi: 10.31699/ijcpe.2013.3.6.